$12^{th}$ International Conference on Fracture Mechanics of Concrete and Concrete Structures
FraMCoS-12
B.L.A. Pichler, Ch. Hellmich, P. Preinstorfer (Eds)

https://doi.org/10.21012/FC12.1372
PL5

# FRACTURE INVESTIGATION IN HETEROGENEOUS POROUS MATERIALS ACROSS SCALES

**RYAN NIELSEN** [1] **AND PANIA NEWELL**[1*]

[1] The University of Utah
Salt Lake City, Utah, USA
e-mail: pania.newell@utah.edu,
https://newell.mech.utah.edu/

**Key words:** Phase-Field fracture, FEniCSx, Homogenization

**Abstract.** Heterogeneous porous materials, characterized by variations in porosity and pore distribution, exhibit complex mechanical behavior, particularly when subjected to fracture. Here, we present a numerical method using phase-field fracture technique in FEniCSX to study how changes in porosity and pore distribution impact the fracture behavior of cementitious materials. The results demonstrate that not only porosity but also pore morphology plays a significant role in fracture propagation and the overall response of cement-mortar. These findings highlight the importance of considering both the quantity and spatial arrangement of pores when assessing the mechanical performance and durability of cement-based materials.

## 1 INTRODUCTION

Porous materials have played a transformative role in advancing civilization, driving progress across various scientific and engineering disciplines. From ancient water filtration techniques [26] to modern applications in designing efficient and sustainable infrastructure [18], porous materials have consistently demonstrated their uniqueness and resilience in shaping the world around us. Cement-based materials, as a class of porous materials, are commonly used materials in infrastructures due to their strength, durability, and overall performance. For example, concrete has complicated and complex pore distribution with varied pore shapes, and pores ranging in size from microscopic to macroscopic [16, 23, 30]. Such complex morphology, heterogeneity and variability in their porous structure pose challenges in optimizing their response for different applications and under different conditions.

To address these challenges, numerous studies, both experimental and numerical, have been conducted to understand the role of underlying pore morphology and the impact on the overall behavior of the material. Experimental approaches, including imaging techniques such as X-ray tomography and scanning electron microscopy (SEM), allow for detailed analysis of pore morphology, size distribution, and connectivity [21, 28]. These methods provide valuable insights into how the material's pore structure influences its mechanical and permeability properties. Additionally, numerical modeling, including finite element analysis (FEA), has been employed to simulate the behavior of cement-based materials under various conditions, helping to predict their response to environmental factors and mechanical loading [8, 12]. Overall, many researchers have highlighted the variations in pore size, distribution, and connectivity can significantly affect the material's mechanical properties, permeability, and durability [2, 17, 27, 29].

With recent advancements in additive manufacturing, the goal is to design materials with controlled porosity, including greener and safer cement-based structures. Achieving this requires a thorough understanding of the pore-property relationships in these heterogeneous systems, which is essential for developing tailored porous materials with desired properties. Therefore, this paper presents a numerical assessment of the role of the underlying porous structure in cementitious materials.

## 2 METHODOLOGY

To determine how variation of microscale pore morphology in concrete affects its macroscale fracture behavior, a two-step numerical process is implemented.

The pairing of numerical homogenization with phase-field modeling allows one to circumvent the intractable task of capturing microscale features at the macroscale and solving a finite element boundary value problem with a high element count. Instead, anisotropic constitutive effects that capture microscale heterogeneity are linked to a macroscopic model through an effective constitutive tensor, enabling phase-field fracture to model fracture propagation at larger scales while preserving information from smaller length scales.

As shown in Figure 1, the first step is to capture the effective or macroscale constitutive behavior of the concrete body using numerical asymptotic homogenization. This is accomplished by solving a boundary value problem over the smallest repeating unit of the underlying periodic structure. This microscopic unit is referred to as the Representative Volume Element (RVE).

The second step of this methodology is to solve for the fracture behavior corresponding to the loading scenario of the body. To achieve this, phase-field or diffusive modeling is employed. This approach is based on a variational formulation of Griffith's energy balance, where the crack is represented as a scalar damage variable, $\phi$. The effective constitutive tensor, $\bar{C}$, computed through numerical homogenization, is then used in the strain energy component of the energy balance formulation at the macroscopic level.

In this work, we implemented the aforementioned methodology in FEniCSx and analyzed the resulting fracture behavior for the classical problem of a single-edge crack plate under tension. To investigate the impact of the underlying pore morphology on the overall fracture behavior, several cases with varying porosity and pore distributions were considered.

### 2.1 Homogenization

Asymptotic homogenization is based on three assumptions [14, 15, 19, 25]. First, it is assumed that a large separation in scale exists between the microscale heterogeneity, the length scale of the RVE, and the macroscale feature of a given domain. Secondly, the displacement field is assumed to be a two-component field consisting of a periodic microscale component, $u^1$, and a macroscale component, $u^0$, which is assumed to be constant over the length scale of the RVE. Correspondingly, the strain field, $\epsilon$, defined as the symmetric portion of the displacement gradient, is also composed of both a periodic, $\epsilon^1$, and constant component, $\epsilon^0$. This yields the following relation:

$$u(x) = u^0 + u^1(x) = \epsilon^0 x + u^1(x) \quad (1)$$

Lastly, it is assumed that the macroscale strain energy due to loading is equal to the strain energy over the RVE.

$$< \sigma(x) : \epsilon(x) > = < \sigma(x) >< \epsilon(x) > \quad (2)$$

where

$$< f > = \frac{1}{\Omega_{RVE}} \int_{\Omega_{RVE}} f d\Omega_{RVE} \quad (3)$$

and

$$\sigma(x) = C(x) : (\epsilon^1(x) + \epsilon^0) \quad (4)$$

Defining a local boundary value problem over the domain of the RVE, we prescribe $\epsilon^0$ as unit strain tensors corresponding to each unique

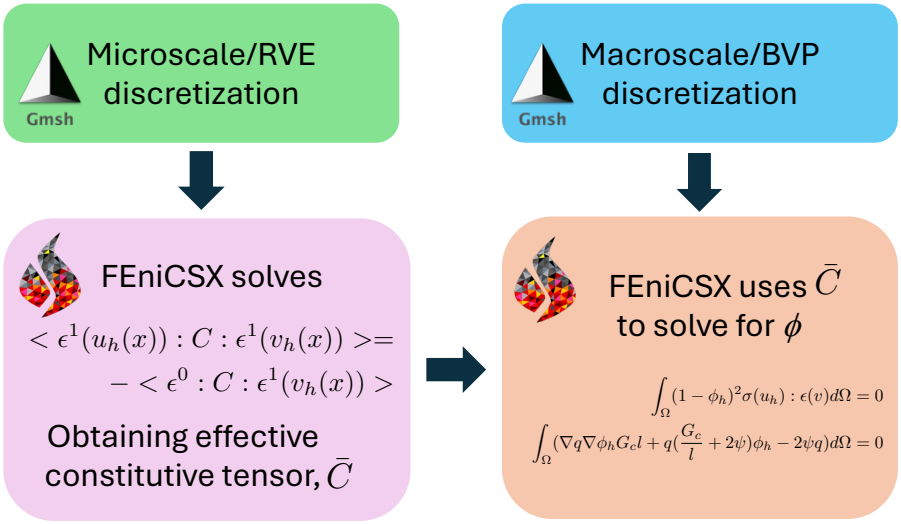


**Figure 1**: Flowchart of the approach used in this study.

component of $\bar{C}$. In two dimensions, this requires unit strain tensors defined along each of the kl directions, where $\epsilon^0_{kl} = 1$. We therefore define the weak formulation of the boundary value problem over the RVE as,

$$< \epsilon^1(u_h(x)) : C : \epsilon^1(v_h(x)) >= - < \epsilon^0 : C : \epsilon^1(v_h(x)) > \quad (5)$$

where $u_h$ and $v_h$ are the corresponding periodic trial and test functions.

Using the Hill-Mandel condition from Equation 2, we compute $\bar{C}$ from the relation,

$$\bar{C}_{ijkl} =< C_{ijkl} - C_{ijmn} \frac{\partial u^{kl}_{hm}}{\partial x_n} > \quad (6)$$

## 2.2 Phase-field

While stress intensity factor-based fracture mechanics methods analyze BVP in which the crack is defined as part of the domain boundary, the phase-field method is based on Griffith's energy balance, $G_c = \psi$ [10], where $\psi$ is the strain energy density of a cracked body under loading and $G_c$ is the critical energy release rate. This can be rewritten as an energy functional by replacing the discontinuity in the domain with a separate scalar field variable, $\phi$ [4, 7, 9, 13].

$$\int_\Omega d(\phi)\sigma : \epsilon \partial\Omega + \frac{1}{2}\int_\Omega G_c(\frac{1}{l}(1-\phi)^2 + l|\nabla\phi|^2)\partial\Omega, \quad (7)$$

This "crack identifier" takes a value of 1 at the crack location and smoothly transitions to 0 at points farther from the crack. The rate of this transition is controlled by the length-scale term, $l$. Further derivations yield the weak form of a coupled system of equations as,

$$\int_\Omega (1-\phi_h)^2 \sigma(u_h) : \epsilon(v) d\Omega = 0 \quad (8)$$

$$\int_\Omega (\nabla q \nabla \phi_h G_c l + q(\frac{G_c}{l} + 2\psi)\phi_h - 2\psi q) d\Omega = 0 \quad (9)$$

It should be noted that the test functions corresponding to trial functions $u_h$ and $\phi_h$ are $v$ and $q$, respectively [20].

## 2.3 Case studies

As shown in Figure 2, this study used the classical benchmark problem of a single-edge crack plate under tension. The material was assumed to have a porous microstructure, with material properties of concrete.

To investigate the role of porosity and variation in pore morphology, eight representative

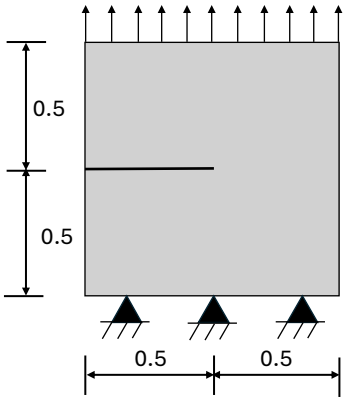


**Figure 2**: Schematic of a single-edge crack plate under tension. Dirichlet boundary conditions prescribed along bottom and top edges.

volume elements (RVEs), each exhibiting a distinct microscopic porous structure of hardened cement paste, the primary matrix within concrete at the microscale, were examined. As shown in Figure 3, two sets of four RVEs with different pore distributions were selected while porosity remains constant (i.e., 20 and 30%). It should be noted that even though any changes in the underlying porous structure typically affect $G_c$, for simplicity, this value was kept constant in this study.

To generate these morphologies, pore sizes and locations were randomly computed using Python's Random libraries. This data was then used to create periodic finite element meshes in Gmsh [11]. For discretizing the RVE, triangular elements with sufficiently small sizes were employed. These meshes were then used to solve the constitutive tensor, $\bar{C}$ using the open-sourced finite element solver, FEniCS [1, 3]. Material properties for the hardened cement paste matrix were computed from homogenization of the nanoscale mixture of cementitious material with 13.18% capillary pores. This nanoscale porosity is only represented at the microscale as the homogenized mixture. The microscale hardened cement paste was then homogenized to include a mixture of 65% sand [22, 24]. This mixture then served as the solid matrix for the RVEs defined above. The boundary value problems were defined to constrain displacement as periodic and unit strain body loads were prescribed. To remove rigid body translations from the problem, $< u_h >= 0$ was enforced using Lagrange multipliers as described by Bleyer [6]. The resulting solutions were then used to compute $\bar{C}$ from Equation 6.

One the $\bar{C}$ is determined, the macroscopic single-edge crack plate can be solved numerically. To accomplish this, the domain is discretized using Gmsh with linear quadrilateral elements, where the element size is determined by half the length of the $l$ term in Equation 9. The $\sigma$ and $\psi$ terms in Equations 8 and 9 are computed using the effective constitutive tensors, $\bar{C}$ for each RVE. Dirichlet boundary conditions are applied to the bottom and top edges of the plate. The displacement on the bottom edge is fixed in both directions, while increasing displacements along the top edge are prescribed to induce tensile stress fields within the domain. Phase-field formulations are solved in FEniCSx [5], an extension of the legacy FEniCS solver with enhanced functionality for quadrilateral meshes.

## 3 RESULTS

To evaluate the structural effect of pore morphology variation for a given porosity, reaction forces occurring at the fixed bottom edge vs the increasing displacement prescribed along the top edge of the plate are compared.

One can observe from Figure 4(a) that higher porosity reduces the maximum force, while the materials experience greater displacement. This is primarily due to the reduced stiffness

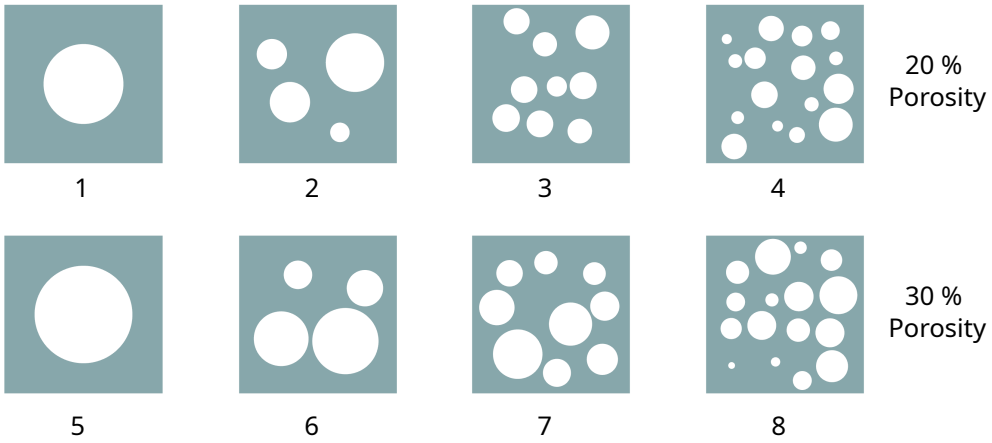


**Figure 3**: Eight selected RVEs to represent variation in the microscale pore morphology of concrete.

of the material, as increased porosity leads to a decrease in the effective load-bearing capacity, allowing for larger deformations under the same applied force. Moreover, as one can see from Figure 4(b), for the same porosity, the morphology also influences the overall load-displacement curve. Specifically, an increase in pore density, while keeping porosity constant, results in a lower maximum force and higher displacement. This can be explained by the fact that variations in morphology can lead to different patterns of local yielding and strain localization, ultimately modifying the material's response to applied loads.

To illustrate the effect of microscale pore morphology on macroscale crack propagation, snapshots of all RVEs with 30% porosity at different displacements are shown in Figure 5. As shown, the crack propagation is clearly influenced by the underlying morphology. Specifically, for the single-pore case, the crack propagates further at a given load compared to all other morphologies. Additionally, clear distinctions are observed among the different cases, even though they all share the same porosity value.

## 4 CONCLUSIONS

In summary, the results highlight the role of both porosity and pore morphology in influencing crack propagation behavior. While higher porosity reduces peak force and increases displacement, the specific morphology further impact the material's response. The observed distinctions in crack propagation across different morphologies, despite sharing the same porosity value, highlight the complex interplay between structure and mechanical performance at the microscale. This insights are important as they enable the design of more durable and efficient materials with tailored mechanical properties for various engineering and scientific applications.

## 5 ACKNOWLEDGMENTS

The authors would like to thank the organizer of the conference

## REFERENCES

[1] M. E. Rognes A. Logg, K. B. Ølgaard and G. N. Wells. FFC: the FEniCS form compiler. In K.-A. Mardal A. Logg and G. N. Wells, editors, *Automated Solution of Differential Equations by the Finite Element Method*, volume 84 of *Lecture Notes in Computational Science and Engineering*, chapter 11. Springer, 2012.

[2] B. Abali, B. E.and Vazic and P. Newell. Influence of microstructure on size effect for metamaterials applied in composite structures. *Mechanics Research Communications*, 122:103877, 2022.

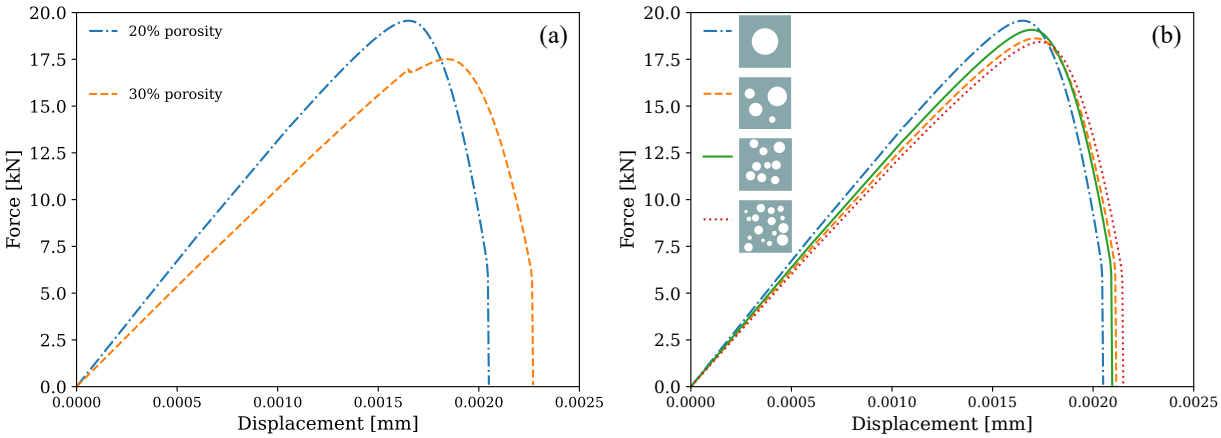


**Figure 4**: Reaction force vs displacement for single-edge crack plate in tension for (a) single pore RVE with different porosity values, (b) RVEs with 20% porosity.

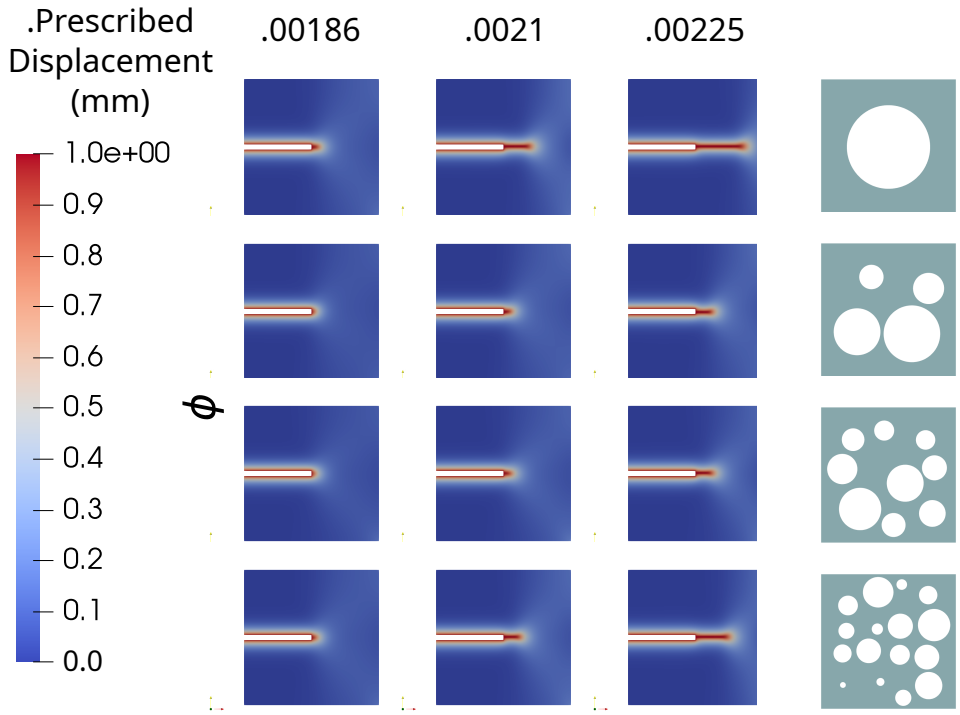


**Figure 5**: Crack propagation comparisons for all pore morphologies of 30%.

[3] Martin S. Alnaes, Jan Blechta, Johan Hake, August Johansson, Benjamin Kehlet, Anders Logg, Chris N. Richardson, Johannes Ring, Marie E. Rognes, and Garth N. Wells. The FEniCS project version 1.5. *Archive of Numerical Software*, 3, 2015.

[4] Luigi Ambrosio and Vincenzo Maria Tortorelli. On the approximation of free discontinuity problems. 1992.

[5] Igor A. Baratta, Joseph P. Dean, Jørgen S. Dokken, Michal Habera, Jack S. Hale, Chris N. Richardson, Marie E. Rognes, Matthew W. Scroggs, Nathan Sime, and Garth N. Wells. DOLFINx: the next generation FEniCS problem solving environment. preprint, 2023.

[6] Jeremy Bleyer. *Numerical Tours of Computational Mechanics with FEniCS*, 2018.

[7] Blaise Bourdin, Gilles A Francfort, and Jean-Jacques Marigo. The variational approach to fracture. *Journal of elasticity*, 91(1):5–148, 2008.

[8] Xin Cheng, Jin Xia, Wei-li Wang, Shijie Jin, Nan Huang, and Wei-liang Jin. Numerical modeling of the effect of concrete porosity evolution on electrochemical chloride removal from concrete structures. *Construction and Building Materials*, 267:120929, 2021.

[9] G.A. Francfort and J.-J. Marigo. Revisiting brittle fracture as an energy minimization problem. *Journal of the Mechanics and Physics of Solids*, 46(8):1319–1342, 1998.

[10] Emmanuel E Gdoutos. *Fracture mechanics: an introduction*, volume 263. Springer Nature, 2020.

[11] Christophe Geuzaine and J-F Remacle. Gmsh: a three-dimensional finite element mesh generator with built-in pre-and post-processing facilities. *International Journal for Numerical Methods in Engineering*, 79(11):1309–1331, 2008.

[12] Meschke Günther and Grasberger Stefan. Numerical modeling of coupled hygromechanical degradation of cementitious materials. *Journal of Engineering Mechanics*, 129(4):383–392, 2024/12/21 2003.

[13] Bang He, Louis Schuler, and Pania Newell. A numerical-homogenization based phase-field fracture modeling of linear elastic heterogeneous porous media. *Computational Materials Science*, 176:109519, 2020.

[14] R. Hill. A self-consistent mechanics of composite materials. *Journal of the Mechanics and Physics of Solids*, 13(4):213–222, 1965.

[15] Scott J Hollister and Noboru Kikuchi. A comparison of homogenization and standard mechanics analyses for periodic porous composites. *Computational mechanics*, 10(2):73–95, 1992.

[16] R. Kumar and B. Bhattacharjee. Porosity, pore size distribution and in situ strength of concrete. *Cement and Concrete Research*, 33(1):155–164, 2003.

[17] B. Liguori, Y. Song, J. W. Zhou, Z. N. Bian, and G. Z. Dai. Pore structure characterization of hardened cement paste by multiple methods. *Advances in Materials Science and Engineering*, 2019:3726953, 2019.

[18] Ippei Maruyama, Jiří Rymeš, Abudushalamu Aili, Shohei Sawada, Osamu Kontani, Shinya Ueda, and Ryu Shimamoto. Long-term use of modern portland cement concrete: The impact of altobermorite formation. *Materials & Design*, 198:109297, 2021.

[19] J.C. Michel, H. Moulinec, and P. Suquet. Effective properties of composite materials with periodic microstructure: a computational approach. *Computer Methods in Applied Mechanics and Engineering*, 172(1):109–143, 1999.

[20] Christian Miehe, Fabian Welschinger, and Martina Hofacker. Thermodynamically consistent phase-field models of fracture: Variational principles and multi-field fe implementations. *International journal for numerical methods in engineering*, 83(10):1273–1311, 2010.

[21] Nadezda Prochukhan, Aran Rafferty, Megan Canavan, Dermot Daly, Andrew Selkirk, Saranya Rameshkumar, and Michael A. Morris. Development and application of a 3d image analysis strategy for focused ion beam – scanning electron microscopy tomography of porous soft materials. *Microscopy Research and Technique*, 87(6):1335–1347, 2024.

[22] Simon Schmid, Jithender J Timothy, Elena Woydich, Jochen Kollofrath, and Christian U Grosse. Comparison of methods for estimating youngâs moduli of mortar specimens. *Scientific Reports*, 14(1):14198, 2024.

[23] Wei She, Guotang Zhao, Degou Cai, Jinyang Jiang, and Xiaoyu Cao. Numerical study on the effect of pore shapes on the thermal behaviors of cellular concrete. *Construction and Building Materials*, 163:113–121, 2018.

[24] Peter Simeonov and Shuaib Ahmad. Effect of transition zone on the elastic behavior of cement-based composites. *Cement and Concrete research*, 25(1):165–176, 1995.

[25] Pierre Suquet. Elements of homogenization for inelastic solid mechanics. *Homogenization techniques for composite media*, 272:193–278, 1987.

[26] Kenneth Barnett Tankersley, Nicholas P. Dunning, Christopher Carr, David L. Lentz, and Vernon L. Scarborough. Zeolite water purification at tikal, an ancient maya city in guatemala. *Scientific Reports*, 10(1):18021, 2020.

[27] Bozo Vazic and Pania Newell. Towards the design of nature-inspired materials: Impact of complex pore morphologies via higher-order homogenization. *Mechanics of Materials*, 181:104641, 2023.

[28] Dorthe Wildenschild and Adrian P. Sheppard. X-ray imaging and analysis techniques for quantifying pore-scale structure and processes in subsurface porous medium systems. *Advances in Water Resources*, 51:217–246, 2013.

[29] Jianzhuang Xiao, Zhenyuan Lv, Zhenhua Duan, and Chuanzeng Zhang. Pore structure characteristics, modulation and its effect on concrete properties: A review. *Construction and Building Materials*, 397:132430, 2023.

[30] He Yang, Yun Jia, Jianfu Shao, and Christophe Pontiroli. Numerical analysis of concrete under a wide range of stress and with different saturation condition. *Materials and Structures*, 48:295–306, 2015.